TABLE 2
Cumulative Washout of Myocardial Radioactive Metabolites

Dog no.	BMIPP (Backdiffusion)	Alpha-oxidation metabolite	Intermediate metabolites	Full metabolites
1	17.9	33.5	40.6	8.0
2	21.3	29.9	39.2	9.6
3	21.6	20.5	21.5	36.4
4	36.7	25.7	36.2	1.4
5	24.4	23.2	26.5	25.9
Average (1 s.d.)	24.4 (7.3)	26.6 (5.2)	32.8 (8.4)	16.3 (14.4)

dial interventions to clarify clinical usefulness of BMIPP as an agent for assessing myocardial fatty acid metabolism.

ACKNOWLEDGMENT

We thank Nihon Medi-Physics Co. Ltd. (Tokyo, Japan) for its generous donations of BMIPP, IPPA, IPDA and AMIPT.

REFERENCES

1. Knapp FF Jr, Goodman MM, Ambrose KR, et al. The development of radioiodinated 3-metyl-branched fatty acids for evaluation of myocardial disease by single photon techniques. In: van del Wall EE ed. *Noninvasive imaging of cardiac metabolism.* Dordrecht: Martius Nijhoff Publishers; 1987:159–201.
2. Fujibayashi, Y, Yonekura Y, Kawai K, et al. Basic studies on ^{123}I-beta-methyl-*p*-iodophenylpentadecanoic acid (BMIPP) for myocardial functional diagnosis: effect of beta-oxidation inhibitor. *Jpn J Nucl Med* 1988;25:1131–1135.
3. Kawamoto M, Tamaki N, Yonekura Y, et al. Combined study with ^{123}I fatty acid and ^{201}Tl to assess ischemic myocardium: comparison with thallium redistribution and glucose metabolism. *Ann Nucl Med* 1994;8:47–54.
4. Takeishi Y, Sukekawa H, Sakurai T, et al. Noninvasive identification of anthracycline cardiotoxicity: comparison of ^{123}I-MIBG and ^{123}I-BMIPP imaging. *Ann Nucl Med* 1994;8:177–182.
5. Som P, Wang GJ, Oster ZH, et al. Myocardial uptake of cocaine and effects of cocaine on myocardial substrate utilization and perfusion in hypertensive rats. *Ann Nucl Med* 1993;7:SII-19–SII-26.
6. Kurata C, Tawarahara K, Okayama K, et al. Myocardial imaging with radioiodinated beta-methyl-branched fatty acid in cardiomyopathy. *Ann Nucl Med* 1993;7:SII-27–SII-33.
7. Nisahimura T, Uehara T, Shimonagata T, et al. Clinical experience of ^{123}I-BMIPP myocardial imaging for myocardial infarction and hypertrophic cardiomyopathy. *Annal Nucl Med* 1993;7:SII-35–SII-39.
8. Tamaki N, Kawamoto M, Yonekura Y, et al. Assessment of fatty acid metabolism using ^{123}I branched fatty acid: comparison with positron emission tomography. *Ann Nucl Med* 1993;7:SII-41–SII-47.
9. Kropp J, Jörgens M, Glänzer KP, et al. Evaluation of ischemia and myocardial viability in patients with coronary artery disease (CAD) with iodine-123-labeled 15-(p-iodophenyl)-3-R,S-methylpentadecanoic acid (BMIPP). *Ann Nucl Med* 1993;7:SII-93–SII-100.
10. Franken PR, Geeter DF, Dendale P, et al. Abnormal free fatty acid uptake in subacute myocardial infarction after coronary thrombolysis: correlation with wall motion and inotropic reserve. *J Nucl Med* 1994;35:1758–1765.
11. Geeter DF, Franken PR, Knapp FF Jr, Bossuyt A. Relationship between blood flow and fatty acid metabolism in subacute myocardial infarction: a study by means of ^{99m}Tc-sestamibi and ^{123}I-meta-methyl-iodo-phenyl mentadecanoic acid. *Eur J Nucl Med* 1994;21:283–291.
12. Matsunari I, Saga T, Taki J. Relationship between various parameters derived from ^{123}I-labeled beta-methyl-branched fatty acid whole-body scintigraphy and left ventricular ejection fraction in patients with ischemic heart disease. *Nucl Med Commun* 1994;15:685–689.
13. Ohtsuki K, Sugihara H, Umamoto I, et al. Clinical evaluation of hypertrophic cardiomyopathy by myocardial scintigraphy using ^{123}I-labeled 15-(p-iodophenyl)-3-R,S-methylpentadecanoic acid (^{123}I-BMIPP). *Nucl Med Commun* 1994;15:441–447.
14. Kawamoto M, Tamaki N, Yonekura Y, et al. Combined study with ^{123}I-fatty acid and thallium-201 to assess ischemic myocardium: comparison with thallium redistribution and glucose metabolism. *Ann Nucl Med* 1994;8:47–54.
15. Tawarahara K, Kurata C, Taguchi T, et al. Simultaneous dual myocardial imaging with ^{123}I-beta-methyl iodophenyl-pentadecanoic acid (BMIPP) and ^{201}Tl in patients with coronary heart disease. *Jpn Circ J* 1994;58:107–115.
16. Goodman MM, Knapp FF Jr, Callahan AP, Ferren LA. A new, well-retained myocardial imaging agent: radioiodinated 15-(*p*-iodophenyl)-6-tellurapentadecanoic acid. *J Nucl Med* 1982;23:904–908.
17. Yamamichi Y, Kusuoka H, Morishita K, et al. Metabolism of ^{123}I-labeled 15-(p-iodophenyl)-3-(R,S)-methylpentadecanoic acid (BMIPP) in perfused rat hearts. *J Nucl Med* 1995;36:1043–1050.
18. Okuda K, Nohara R, Fujita M, et al. Technetium-99m-pyrophosphate uptake as an indicator of myocardial injury without infarct. *J Nucl Med* 1994;35:1366–1370.
19. Folch J, Lees M. Proteolipides, a new type of tissue lipoproteins. *J Biol Chem* 1951;191:807–817.
20. Bianco JA, Elmaleh DR, Leppo JA, et al. Effect of glucose and insulin infusion on the myocardial extraction of a radioiodinated methyl-substituted fatty acid. *Eur J Nucl Med* 1986;12:120–124.
21. Otto C, Brown LE, Wieland DM, Beierwaltes. Radioiodinated fatty acids for myocardial imaging: effects of chain length. *J Nucl Med* 1981;22:613–618.
22. Nishimura T, Sago M, Kihara K, et al. Fatty acid myocardial imaging using ^{123}I-β-methyl-iodophenyl pentadecanoic acid (BMIPP): comparison of myocardial perfusion and fatty acid utilization in canine myocardial infaction (occlusion and reperfusion model). *Eur J Nucl Med* 1989;15:341–345.
23. Matsunari I, Ichiyanagi K, Taki J, et al. Evaluation of early kinetics of ^{123}I-BMIPP in patients with ischemic heart disease. *Jpn J Nucl Med* 1993;30:1445–1450.25.
24. Kobayashi H, Asano R, Oka T, et al. Simultaneous evaluation of myocardial perfusion and fatty acid metabolism using dynamic SPECT with single injection of ^{123}I-15-(p-iodophenyl)-3-methyl pentadecanoic acid (BMIPP). *Jpn J Nucl Med* 1995;32:19–29.

Ischemic and Reperfused Myocardium Detected with Technetium-99m-Nitroimidazole

Kazuki Fukuchi, Hideo Kusuoka, Yoshiyuki Watanabe, Toshiyuki Fujiwara and Tsunehiko Nishimura

Division of Tracer Kinetics, Biomedical Research Center, Osaka University Medical School, Suita, Osaka, Japan

To evaluate the utility of ^{99m}Tc-labeled nitroimidazole (BMS) in the detection of ischemic or reperfused myocardium, we performed dual-tracer autoradiography with BMS and [^{125}I]iodoantipyrine (IAP). **Methods:** In open-chest rats, the left coronary artery was ligated to produce 15- or 60-min ischemia followed by reperfusion or 60-min ischemia without reperfusion. BMS was injected just before ligation, 1 min before reperfusion or 15 min after reperfusion. **Results:** In the area at risk, regional myocardial blood flow (rMBF) evaluated by IAP recovered to the level in the nonischemic septum in all hearts, except in 60-min occlusion without reperfusion. In myocardium reperfused after 15-min ischemia (stunned), normalized BMS uptake (%BMS) in the area at risk was significantly increased only when BMS was injected before ischemia. When BMS was injected before 60-min ischemia or just before reperfusion, %BMS was significantly higher at the marginal zone of infarction than in the infarcted area. In contrast, %BMS was significantly lower in the infarcted area when BMS was injected during reperfusion. After 60 min of occlusion without reperfusion (permanent occlusion), rMBF in the area at risk was significantly decreased as was %BMS. In the peripheral zone of the area at risk, rMBF was significantly reduced, but %BMS was significantly increased. **Conclusion:** BMS images stunned myocardium only when it is injected before ischemia, while it images the area at risk subjected to prolonged ischemia when it is injected up to the time of reperfusion. The infarcted area can be negatively visualized when BMS is injected after reperfusion.

Key Words: technetium-99m-nitroimidazole; ischemia; reperfusion

J Nucl Med 1996; 37:761–766

Received Apr. 3, 1995; revision accepted Sept. 20, 1995.

For correspondence and reprints contact: Kazuki Fukuchi, MD, Division of Tracer Kinetics, Biomedical Research Center, Osaka University Medical School, Yamada-oka 2-2, Suita, Osaka, 565 Japan.

Preservation of ischemic but viable myocardium is one of the major goals of therapy for myocardial infarction and unstable

angina. Appropriate and timely clinical intervention is necessary to restore tissue oxygenation to prevent loss of function or life. Myocardial reperfusion can be achieved by thrombolytic therapy or early bypass surgery. Since reperfusion has become a common treatment for acute myocardial infarction, it is necessary to develop imaging techniques that can be used to determine the success of reperfusion and to distinguish reperfused myocardium from nonreperfused myocardium or infarction. Nitroimidazole was developed as a new radiopharmaceutical which indicates the state of tissue oxygenation (*1,2*). It is a radiolabeled agent that undergoes reduction within cells, forming reactive intermediates, depending on the intercellular oxygen concentration (*3*). Fluorine-18 fluoro-misonidazole and [^{131}I]iodovinyl-misonidazole have already been used to detect myocardial hypoxia, and the possibility has been suggested of imaging hypoxic tissues using both planar scintigraphy and emission computed tomography (*4–6*).

Recently, we determined the kinetics of a new technetium-labeled hypoxia tracer, propyleneamine oxime-1,2-nitroimidazole (BMS-181321), in ischemic or hypoxic myocardium using isolated perfused rat hearts (*7*). We conducted the present study to investigate whether BMS-181321 (BMS) can be used to detect acute ischemic injury of the in vivo rat heart. Dual-tracer autoradiography was used to characterize the binding of BMS in comparison with myocardial perfusion as measured by [^{125}I]iodoantipyrine (*8,9*).

MATERIALS AND METHODS

Female Sprague-Dawley rats (body weight, 280–320 g) were anesthetized with ether and mechanically ventilated after endotracheal intubation. A left-sided thoracotomy was performed via the fifth intercostal space, and a small incision was made in the pericardium. An adjustable ligature was placed around the left coronary artery near its origin beneath the left atrial appendage using a 6.0 silk suture. Both ends of the suture were then threaded through a polyethylene tube to form a snare loop around the coronary artery which could be closed on pulling the free end of the suture. Reperfusion was performed by releasing the snare loop from the coronary artery. The femoral vein was cannulated with a PE-50 polyethylene tube for the injection of radiopharmaceuticals.

Three types of acute ischemic myocardial damage were produced. In Group 1 (n = 12), the myocardium was reperfused after 15 min of coronary ligation. In Group 2 (n = 12), reperfusion was applied for 30 min after 60 min of coronary ligation, and in Group 3 (n = 8), 60 min of coronary ligation was applied without reperfusion. In all groups, occlusion was confirmed by the observation of development of myocardial cyanosis and lack of contractility in the ischemic region. In six other rats (sham operation group), thoracotomy was performed and a ligature was placed around the left coronary artery, but ischemia was not produced. All experiments were approved by the Animal Research Committee of Osaka University Medical School.

Experimental Protocol

Three different protocols were used to image the myocardium with BMS (Fig. 1). Four of the 12 rats in each of Groups 1 and 2 were used for each protocol.

Protocol 1: One hundred and eleven MBq (3 mCi) BMS were intravenously injected 1 min before coronary ligation, and 185 KBq (5 μCi) ^{125}I-4-iodoantipyrine ([^{125}I]IAP) were injected 30 min after the start of reperfusion.

Protocol 2: BMS was injected at the start of reperfusion and [^{125}I]IAP was injected after 30 min of reperfusion.

Protocol 3: BMS was injected 15 min after the start of reperfusion and [^{125}I]IAP was injected 15 min later.

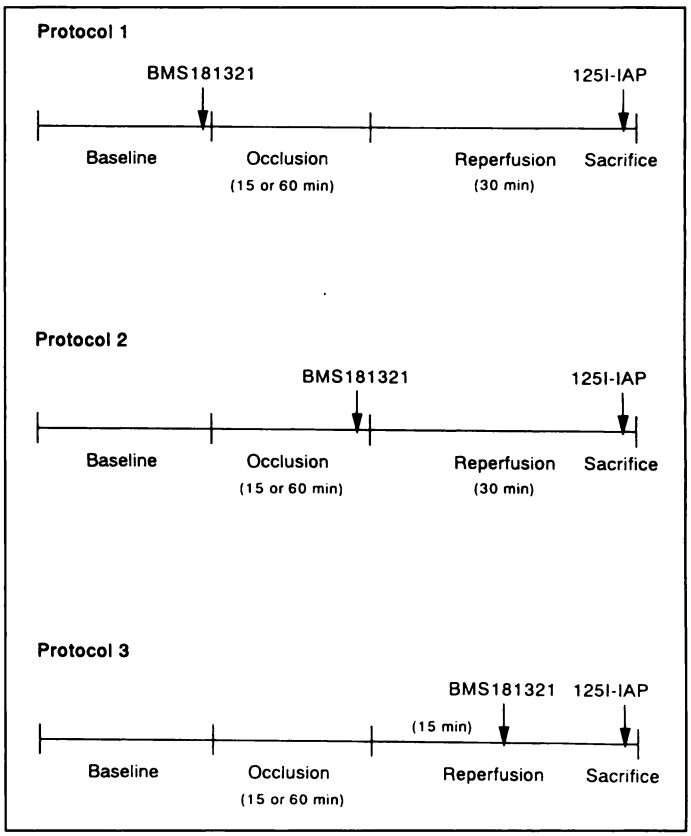

FIGURE 1. Experimental protocols.

In Group 3 (60 min of occlusion without reperfusion), BMS was injected during ligation (45 min after the start of occlusion) and [^{125}I]IAP was injected after 60 min of occlusion.

Autoradiographic method using IAP is suitable for the measurement of regional myocardial blood flow (rMBF), especially in small animals such as rats, because of the excellent spatial resolution it affords. This method is based on the presumption of flow-limited and not diffusion-limited exchange of the tracer between blood and tissue (*10*). The validity of this presumption has been confirmed in the brain, and in the heart it is probably also as valid as flow measurement using microspheres (*9*).

One minute after the injection of [^{125}I]IAP, the rats were killed by injection of saturated KCl, and the heart was rapidly excised and cut at the midline of the left ventricle (LV). The apical half of the heart was frozen in powdered dry ice and cut into 20-μm sections with a cryostat in the direction perpendicular to the longitudinal axis of the LV. The sections at the midventricle were placed on glass cover slips and placed on an imaging plate.

The first autoradiographic exposure was performed for 1 hr to detect the distribution of BMS. After a 7-day waiting period for ^{99m}Tc decay, the second exposure was conducted for 6 hr to obtain an adequate ^{125}I image. It was preliminarily confirmed by single-tracer autoradiography using [^{125}I]IAP that this agent was not visualized under the conditions used for BMS imaging.

The autoradiographic images were analyzed by a computerized imaging analysis system (*11*). To quantitate the myocardial distribution of BMS and [^{125}I]IAP, regions of interest (ROIs) were placed at the interventricular septum (control) and the LV free wall (area at risk). We placed five to six circular ROIs with area of 4 mm^2 in each area. The histological characteristics of each ROI was determined directly by hematoxylin-eosin (H&E) staining, and the corresponding sections in a proximal part of the heart was examined by triphenyltetrazolium chloride staining. The uptakes of BMS and [^{125}I]IAP were normalized by that of the interventricular

septum and expressed as the mean percent uptake of BMS (%BMS) and of [^{125}I]IAP (%IAP), respectively. The %IAP uptake was used as a measure of rMBF.

Histological Examination

In the determination of the infarcted area, the residual heart tissue was rinsed with normal saline and cut into several transverse slices (2–3 mm in thickness) parallel to the atrioventricular groove. The slices were immersed in a 2% solution of 2,3,5-triphenyltetrazolium chloride (TTC) at 37°C for 30 min and then fixed by immersion in a 10% phosphate-buffered formalin solution (pH 7.4). Viable myocardium is stained red by TTC, whereas necrotic myocardium appears pale yellow. This stain has been shown to be a reliable indicator of myocardial infarction (*12*). The TTC-stained slice obtained from the midventricle was photographed and the area of infarction was measured planimetrically. The myocardial tissue used for autoradiography was also sectioned at a thickness of 10–15 μm and stained with H&E stain.

Radiopharmaceutical Preparation

BMS-181321 was prepared from the provided ligand kits as described previously (*13*). The radiochemical purity was 90% as determined by paper chromatography using a Gelman solvent saturation pad developed in diethyl ether. [^{125}I]-4-iodoantipyrine was prepared as described previously (*14*). Briefly, [^{125}I]iodide (50 μl/5 mCi) and nonradioactive 4-bromoantipyrine (5.34 mg, 20 μmole) were mixed in an acidic aqueous solution at 100°C for 15 min. After cooling, the labeled 4-iodoantipyrine was separated from the radioiodide by reversed-phase high performance liquid chromatography (eluent: 45% methanol, flow rate: 5 ml/min, retention time: 72 min). The radiochemical yield was 83.25 MBq (45%, uncorrected for decay). Radiochemical purity of the sample was confirmed by thin-layer chromatography.

Statistical Analysis

Data are expressed as the mean ± s.e.m. Comparison among groups was done using analysis of variance (ANOVA) with a multiple comparison test. Comparison within groups was performed using the paired Student's t-test. Probability of less than 0.05 was considered to indicate a significant difference.

RESULTS

Sham Operation Group

There was no infarction of the LV free wall demonstrated by either TTC or H&E staining. The [^{125}I]IAP uptake was homogeneous in all myocardial regions, and the BMS uptake was also uniform. The relative uptake of BMS (%BMS) and of [^{125}I]IAP (%IAP) for the LV free wall was 101% ± 5% and 98% ± 4%, respectively, and there was no significant difference compared to the uptake for the septum.

Group 1 (Stunned Myocardium)

Myocardium reperfused after a brief period of ischemia is known as stunned myocardium (*15*) and one of its characteristics is the absence of necrosis. In all rats in Group 1, TTC and H&E staining disclosed no infarction of the LV free wall (the area at risk). Figure 2 shows autoradiograms obtained with [^{125}I]IAP and BMS. The uptake of [^{125}I]IAP was uniform for all three protocol (left panels), whereas the distribution of BMS varied with the protocols (right panels). The BMS uptake was significantly elevated in the area at risk when it was injected before ischemia (Protocol 1, Fig. 2A), while the BMS uptake was low when it was injected at the start of reperfusion (Protocol 2, Fig. 2B) or during reperfusion (Protocol 3, Fig. 2C).

Figure 3 summarizes the relative uptake of [^{125}I]IAP and BMS by the LV free wall, i.e., the area at risk. The rMBF values

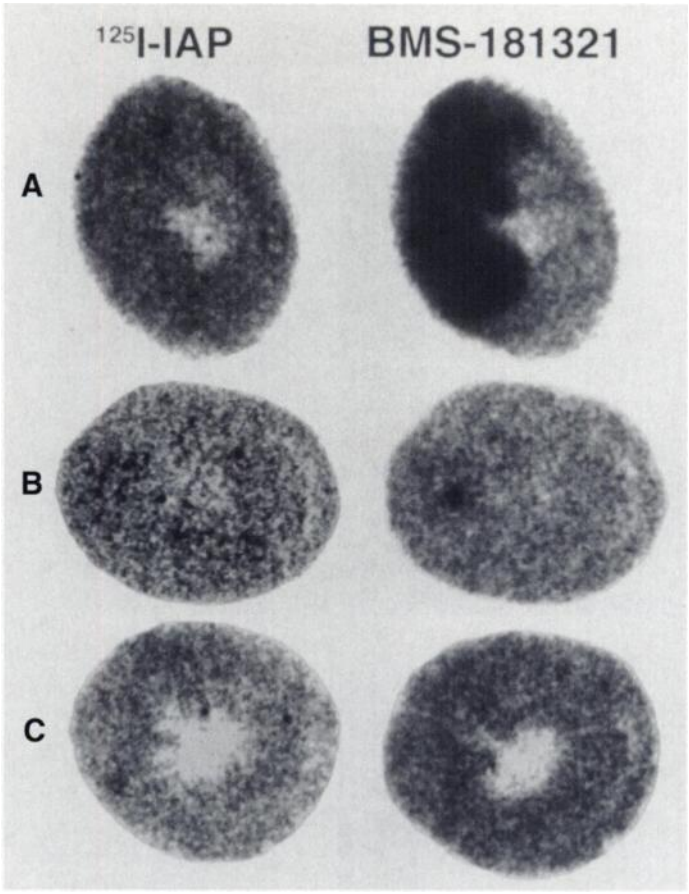

FIGURE 2. Dual-tracer autoradiograms obtained with [^{125}I]iodoantipyrine (IAP) and BMS-181321 (BMS) after 15 min coronary occlusion and reperfusion. (A) BMS was injected before coronary ligation. (B) BMS was injected just before reperfusion. (C) BMS was injected after 15 min of reperfusion.

measured by [^{125}I]IAP were almost identical among the three protocols (103% ± 7% for Protocol 1, 95% ± 3% for Protocol 2, and 104% ± 7% for Protocol 3), and none of them differed from that in the sham-operated group. In contrast, the values for %BMS in the area at risk were significantly different among the three protocols, that in Protocol 1 being significantly higher (790% ± 50%) than that in either of the others (98% ± 1% for Protocol 2 and 108% ± 3% for Protocol 3; both $p < 0.01$). Additionally, BMS uptake by the area at risk in Protocols 2 and 3 was almost identical to that in the sham-operated group. These results indicate that BMS can image stunned myocardium only when it was injected before the ischemic insult, and they are comparable with data obtained in isolated perfused hearts (*7*).

Group 2 (Reperfusion after 60 Minutes of Occlusion)

Reperfusion after 60 min of occlusion resulted in myocardial infarction of the LV free wall (area at risk), as confirmed by TTC and H&E staining. Necrosis was found mainly in the midmyocardial and subepicardial layers with subendocardial sparing (Fig. 4), as reported earlier (*12*).

The uptake of [^{125}I]IAP in the area at risk was uniform for all three protocols (left panels of Fig. 5), as was found in Group 1. In contrast, the distribution of BMS in the infarcted area was quite different from that in the noninfarcted risk area with all three protocols (right panels of Fig. 5). When BMS was injected before ischemia, %BMS was marked in the area at risk, and the uptake for the noninfarcted risk area was significantly larger than that for the infarcted area (Protocol 1, Fig. 5A). When BMS was injected just before reperfusion (Protocol 2), its distribution was similar to that with Protocol 1, but the uptake

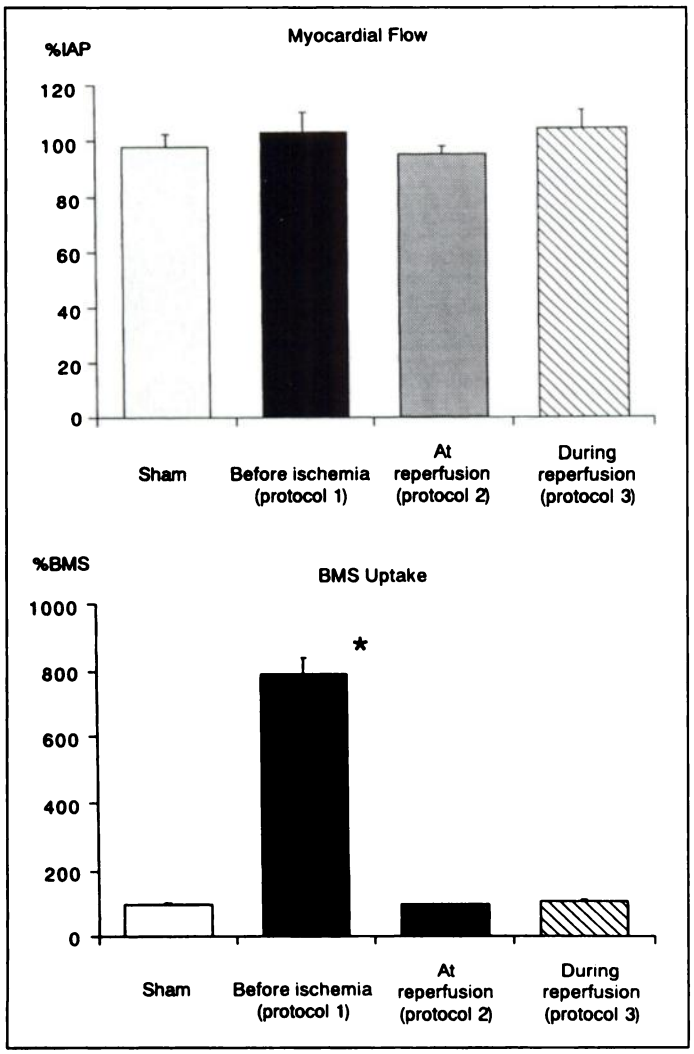

FIGURE 3. Myocardial blood flow and percent uptake of BMS by the area after 15 min of ischemia and reperfusion. Before ischemia, at reperfusion and during reperfusion indicate the times when BMS was injected.

was significantly lower (Fig. 5B). When BMS was injected during reperfusion (Protocol 3), the uptake for the infarcted area was significantly lower than that for the noninfarcted risk area (Fig. 5C).

Figure 6 summarizes the relative uptake of [^{125}I]IAP and BMS for the area at risk. Infarction was confirmed by histological examination. The noninfarcted area in the risk area was determined as the area adjusted to the necrosis in the LV free wall, because the territory fed by the left coronary artery does not vary among rat hearts due to the slight degree of collateral formation (*16*). The rMBF in the infarcted area was almost identical to that in the noninfarcted area for all three protocols

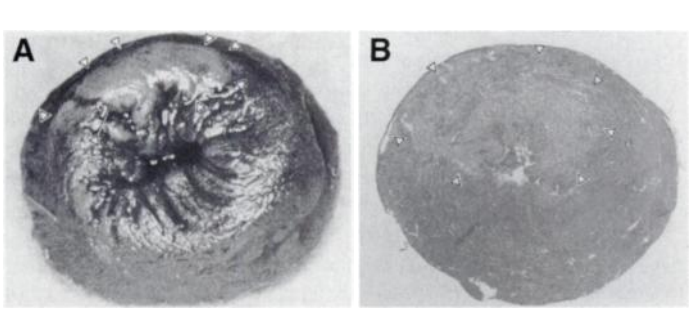

FIGURE 4. Section of a heart reperfused after 60 min of occlusion. (A) TTC staining. (B) H&E staining. Infarction of the infero-lateral left ventricular wall is clearly demonstrated (white arrow heads).

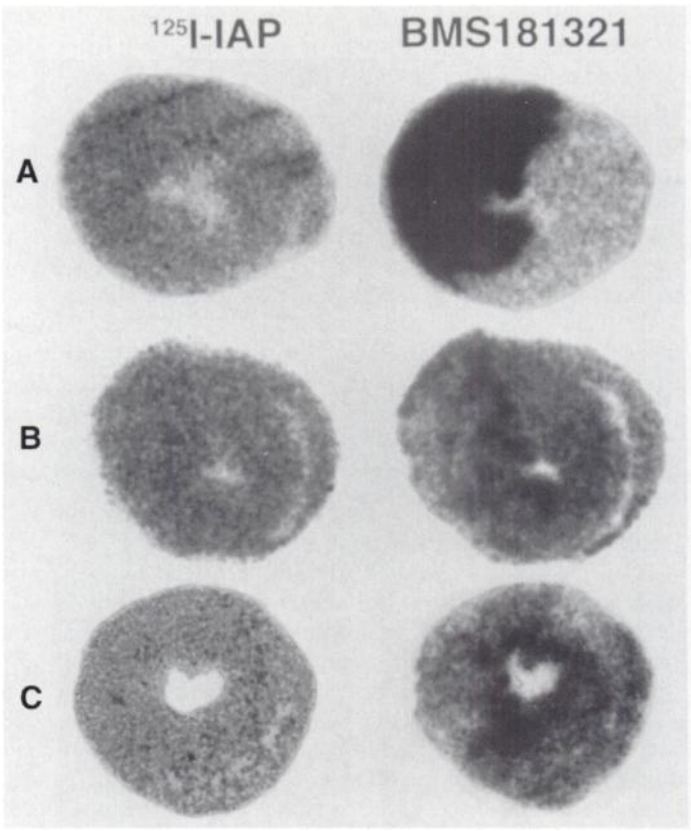

FIGURE 5. Dual-tracer autoradiograms obtained with [^{125}I]IAP and after 60 min of coronary occlusion and reperfusion. (A) BMS was injected before coronary ligation. (B) BMS was injected just before reperfusion. (C) BMS was injected after 15 min of reperfusion.

(121% ± 4% versus 108% ± 5% for Protocol 1; 121% ± 5% versus 109% ± 7% for Protocol 2; and 93% ± 3% versus 92% ± 3% for Protocol 3; all p = ns). On the other hand, %BMS in the noninfarcted risk area was significantly higher than that in the infarcted area when BMS was injected before ischemia or just before reperfusion (956% ± 54% versus 511% ± 43% for Protocol 1, $p < 0.005$; and 235% ± 16% versus 108% ± 7% for Protocol 2, $p < 0.01$). When BMS was injected during reperfusion, its uptake for the infarcted area (67% ± 2%) was lower than that for the noninfarcted area at risk (98% ± 1%, $p < 0.05$).

These results indicate that BMS was retained in the infarcted myocardium when injected before coronary ligation, but that it was not accumulated when injected just before reperfusion. When BMS was injected during reperfusion, its uptake for the infarcted area was lower than that for the septum because the number of the viable cells was decreased in the necrotic area. BMS uptake in the area at risk adjacent to the site of infarction was markedly increased when it was injected before ischemia or at reperfusion.

Group 3 (60 Minutes of Occlusion without Reperfusion)

Coronary occlusion for 60 min without reperfusion caused infarction which was distributed similar to that in Group 2 except a larger extent of infarction.

With 60 min of ischemia and no reperfusion, BMS was also retained only when injected before coronary ligation (data not shown). In contrast, BMS showed different distribution when injected during ischemia (Fig. 7). The distribution of [^{125}I]IAP was homogeneous in the septum (control) and the right ventricular wall. On the other hand, [^{125}I]IAP uptake was almost absent in the area at risk. BMS uptake did not occur in the area

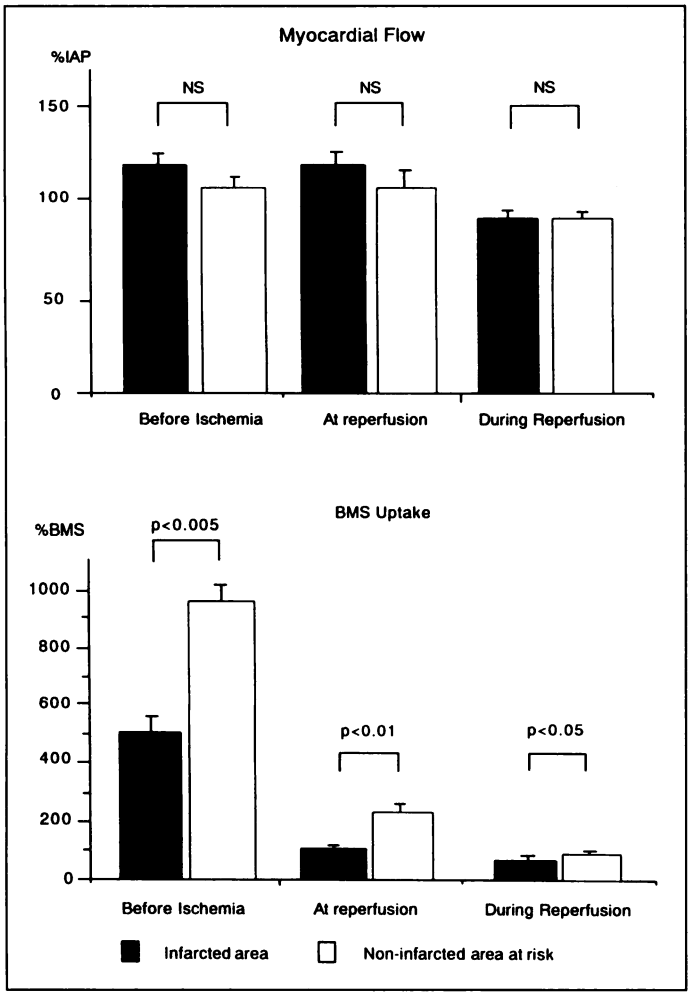

FIGURE 6. Myocardial blood flow and percent uptake of BMS by the area after 60 min of ischemia. Before ischemia, at reperfusion and during reperfusion indicate the times when BMS was injected.

at risk, but it was marked in the marginal zone of the area at risk.

Figure 8 summarizes the relative uptake of [^{125}I]IAP and BMS in the different myocardial regions. The rMBF was reduced to 14% ± 1% in the area at risk, while it was 52% ± 8% in the marginal zone of the area at risk, and both levels were significantly decreased compared to that for the septum ($p < 0.005$ and $p < 0.01$, respectively). %BMS in the area at risk was reduced to 16% ± 4% ($p < 0.01$). In contrast, its uptake by the

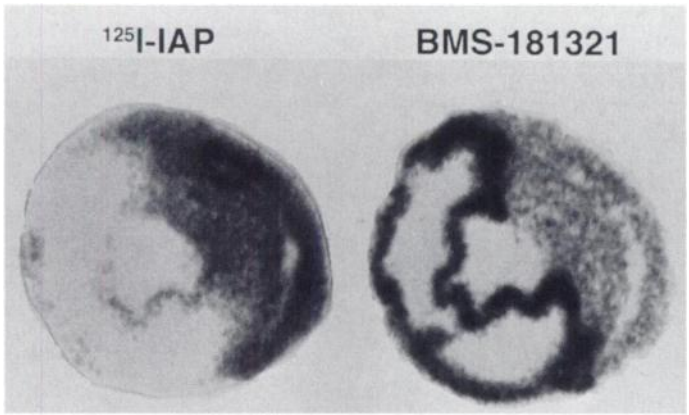

FIGURE 7. Dual-tracer autoradiograms obtained with [^{125}I]IAP and BMS after 60 min of coronary occlusion without reperfusion (permanent occlusion).

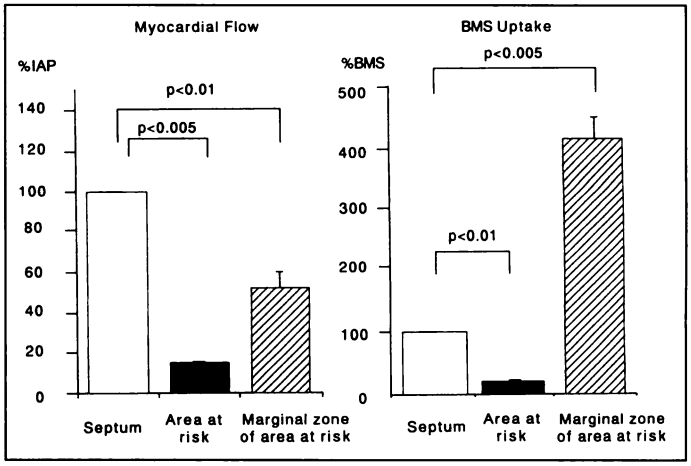

FIGURE 8. Myocardial blood flow and percent uptake of BMS by the area after 60 min of ischemia without reperfusion.

marginal area at risk was significantly increased to 413% ± 36% ($p < 0.005$).

DISCUSSION

The energy for myocardial contraction is mainly supplied through oxidative phosphorylation, and the lack of oxygen due to ischemia or hypoxia naturally causes severe deterioration of cardiac function. Thus, a marker of the imbalance between oxygen supply and demand can provide important metabolic information. Misonidazole and related compounds are metabolically trapped in viable cells as a function of reduced cellular pO2 (*17,18*). BMS, a derivative of misonidazole, was developed to identify hypoxic tissue (*19,20*). This study focused on the applicability of BMS in the detection of the reperfused myocardium after ischemia.

BMS Uptake by Ischemic and Reperfused Myocardium

When BMS was injected before ischemia (Protocol 1), tracer uptake in the area at risk was significantly increased after both 15 min and 60 min of ischemia. In this case, BMS was trapped in the myocardium mechanically and irreversible binding occurred in the area at risk during no-flow ischemia. Once this occurred, reoxygenation and reperfusion did not wash BMS out of the myocardium. With 60 min of ischemia and no reperfusion, BMS was also retained only when it was injected before coronary ligation. In an ischemia-reperfusion canine model, the level of BMS in the ischemic area was reported to be markedly greater than that in the normoxic region (4:1) when it was injected before coronary ligation (*21*). These data and our results suggest that BMS can reveal an ischemic episode after reperfusion when it is administered before the ischemic insult.

When BMS was injected just before the start of reperfusion (Protocol 2), there was significant accumulation in the noninfarcted area at risk compared to that in the septum after 60 min of ischemia. In the peri-infarct region, ischemia may persist for several minutes after reperfusion, and this may have caused the retention of BMS. On the other hand, BMS was not retained in stunned myocardium when it was injected at reperfusion. It is not surprising that the kinetics of BMS observed under these conditions are similar to those in the normoxic region, because stunned myocardium is well perfused and not hypoxic (*15*).

When BMS was injected during reperfusion (Protocol 3), it was not retained by stunned myocardium, as was the case when it was injected just before reperfusion (Protocol 2). Stone et al. (*22*) reported similar results in an open-chest swine model with 40 min of ischemia followed by 100 min of reperfusion. Regional uptake of BMS in the territory of the left coronary

artery was not detected after injection during reperfusion. Following 60 min of ischemia, BMS uptake by the infarcted area was lower than that by the septum, because the number of viable cells was smaller in the necrotic area. These results suggest that enhanced uptake does not occur in the infarcted area because the tissue is already necrotic and therefore lacks the capacity to bind BMS. This explanation is certainly compatible with in vitro observations that binding of BMS to dead cells does not occur (*3,17*). The marginal zone of the area at risk completely recovered from hypoxia with sufficient reperfusion, so BMS was not trapped in this tissue. These data also support the hypothesis that BMS can be trapped only at a certain level of hypoxia which does not cause necrosis, suggesting that it may be used as a metabolic probe for ischemic but viable myocardium.

When BMS was injected during coronary occlusion, its uptake by the area at risk was decreased to 16% of the control level. The rMBF in this area also fell to 14% of the control level, indicating that accumulation of BMS corresponded to rMBF. In the peripheral region of the area at risk, however, the accumulation of BMS was significantly increased despite the low MBF. This finding indicates that hypoxic tissue was present in this region, which was probably perfused by collateral flow from the surrounding normally perfused area. Thus, BMS may possibly be used clinically to identify myocardium which is chronically underperfused but viable (i.e., hibernating).

Clinical Implications

BMS can clearly image ischemic myocardium if it is injected before ischemia. This suggests that BMS may be useful in the detection of ischemia induced by stress such as exercise under circumstances in which the agent can be administered before the onset of ischemia. Myocardial hypoxia is not specifically targeted by flow indicators such as ^{201}Tl and ^{99m}Tc-sestamibi (*23,24*). On the other hand, infarct-avid agents such as ^{99m}Tc-pyrophosphate and ^{111}In-antimyosin antibodies require cellular necrosis to detect the area at risk (*25,26*). Our data demonstrate that BMS study provides information which is different from that provided by these other tracers and may be clinically useful in the identification of hypoxic but potentially salvageable myocardium.

CONCLUSION

In this rat model, BMS can clearly image ischemic myocardium when it is injected before ischemia. Stunned myocardium was not identified by BMS. The area at risk after prolonged ischemia was also imaged when BMS was injected before reperfusion, while the infarcted area could be negatively visualized when it was injected after reperfusion. BMS may be useful in imaging hypoxic but potentially salvageable myocardium.

ACKNOWLEDGMENT

We thank Bristol-Myers Squibb Pharmaceutical Research Institute for providing BMS-181321.

REFERENCES

1. Chapman JD. Hypoxic sensitizers; implications for radiation therapy. *N Engl J Med* 1979;301:1429–1432.
2. Chapman JD, Franko AJ, Sharplin J. A marker for hypoxic cells in tumors with potential clinical applicability. *Br J Cancer* 1981;43:546–550.
3. Martin GV, Caldwell JH, Rasey JS, Grunbaum Z, Cerqueira M, Krohn KA. Enhanced binding of the hypoxic cell marker [^{3}H]fluoromisonidazole in ischemic myocardium. *J Nucl Med* 1989;30:194–201.
4. Koh WJ, Rasey JS, Evans ML, et al. Imaging of hypoxia in human tumors with [^{18}F]fluoromisonidazole. *Int J Radiat Oncol Biol Phys* 1992;22:199–212.
5. Shelton ME, Dence CS, Hwang DR, Welch MJ, Bergmann SR. Myocardial kinetics of fluorine-18 misonidazole: a marker of hypoxic myocardium. *J Nucl Med* 1989;30: 351–358.
6. Martin GV, Biskupiak JE, Caldwell JH, Rasey JS, Krohn KA. Characterization of iodovinylmisonidazole as a marker for myocardial hypoxia. *J Nucl Med* 1993;34:918–924.
7. Kusuoka H, Hashimoto K, Fukuchi K, Nishimura T. Kinetics of a putative hypoxic tissue marker, technetium-99m nitroimidazole (BMS181321), in normoxic, hypoxic, ischemic and stunned myocardium. *J Nucl Med* 1994;35:1371–1376.
8. Krasnow N, Levine HJ, Wagman RJ, Gorlin R. Coronary blood flow measured by [^{131}I]iodo-antipyrine. *Circ Res* 1963;12:58–62.
9. Malsky PM, Vokonas PS, Paul SJ, Robbins SL, Hood WB. Autoradiographic measurement of regional blood flow in normal and ischemic myocardium. *Am J Physiol* 1977;232:H576–H583.
10. Sakurada O, Kennedy C, Jehle J, Brown DJ, Carbin GL, Sokoloff L. Measurement of local cerebral blood flow with iodo[^{14}C]antipyrine. *Am J Physiol* 1978;234:H59–H66.
11. Yanai K, Ryu JH, Watanabe T, Iwata R, Ido T. Receptor autoradiography with ^{11}C and [^{3}H]labeled ligands visualized by imaging plates. *Neuroreport* 1992;3:961–964.
12. Hale SL, Kloner RA. Effect of early coronary artery reperfusion on infarct development in a model of low collateral flow. *Cardiovasc Res* 1987;21:668–673.
13. Linder KE, Chan YW, Cyr JE, Malley MF, Nowotnik DP, Nunn AD. TcO (PnAO-1-(2-nitroimidazole)) [BMS-181321], a new technetium-containing nitroimidazole complex for imaging hypoxia: synthesis, characterization and xanthine oxidase-catalyzed reduction. *J Med Chem* 1994;37:9–17.
14. Robinson GD, Lee AW. Reinvestigation of the preparation of ^{131}I-4-iodoantipyrine from ^{131}I-iodide. *Int J Appl Radiat Isotopes* 1979;30:365–367.
15. Braunwald E, Kloner R. The stunned myocardium: prolonged, postischemic ventricular dysfunction. *Circulation* 1982;66:1146–1149.
16. Hale SL, Vivaldi MT, Kloner RA. Fluoresent microspheres: a new tool for visualization of ischemic myocardium in rats. *Am J Physiol* 1986;251:H863–H868.
17. Rasey JS, Grunbaum Z, Magee S, et al. Characterization of radiolabeled fluoromisonidazole as a probe for hypoxic cells. *Radiat Res* 1987;111:292–304.
18. Chapman JD, Baer K, Lee J. Characteristics of the metabolism-induced binding of misonidazole to hypoxic mammalian cells. *Cancer Res* 1983;43:1523–1528.
19. Chan YW, Linder KE, Jayatilak PG, et al. In-vitro studies on the hypoxic retention of a novel technetium-99m-labeled nitroimidazole in rat heart [Abstract]. *J Nucl Med* 1994;35(Suppl):18P.
20. Rumsey WL, Cyr JE, Raju N, Narra, RK. A novel ^{99m}Tc-labeled nitroheterocycle capable of identification of hypoxia in heart. *Biochem Biophys Res Commun* 1993; 193:1239–1246.
21. Rumsey WL, Patel B, Kuczynski B, et al. SPECT imaging of ischemic myocardium using a novel ^{99m}Tc-nitroimidazole [Abstract]. *Circulation* 1993;88:I-250.
22. Stone CK, Mulnix T, Nickles RJ, Renstrom B, Nellis SH, Liedtke AJ. Specificity of regional myocardial retention of the technetium-99m nitroimidazole BMS-181321 during myocardial ischemia and reperfusion: lack of retention with injection in reperfusion [Abstract]. *Circulation* 1994;90:I-368.
23. Wackers FJ, Berman DS, Maddahi J, et al. Technetium-99m-hexakis 2-methoxyisobutyl isonitrile: human biodistribution, dosimetry, safety and preliminary comparison to thallium-201 for myocardial perfusion imaging. *J Nucl Med* 1989;30:301–311.
24. Gibbons RJ, Verani MS, Behrenbeck T, et al. Feasibility of tomographic ^{99m}Tc-hexakis-2-methoxy-2-methylpropylisonitrile imaging for the assessment of myocardial area at risk and the effect of treatment in acute myocardial infarction. *Circulation* 1989;80:1277–1286.
25. Khaw BA, Strauss HW, Moore R, et al. Myocardial damage delineated by indium-111-antimyosin Fab and technetium-99m-pyrophosphate. *J Nucl Med* 1987;28:76–82.
26. Morguet AJ, Munz DL, Klein HH, et al. Myocardial distribution of indium-111-antimyosin Fab and technetium-99m-sestamibi in experimental nontransmural infarction. *J Nucl Med* 1992;33:223–228.